A Discontinuous Galerkin Method for the Full Two-Fluid Plasma Model

J. Loverich *, U. Shumlak

University of Washington, Aerospace and Energetics Research Program, Seattle, WA 98195-2250

Abstract

A discontinuous Galerkin method for the full two-fluid plasma model is described. The plasma model includes complete electron and ion fluids, which allows charge separation, separate electron and ion temperatures and velocities. Complete Maxwell's equations are used including displacement current. The algorithm is validated by benchmarking against existing plasma algorithms on the GEM Challenge magnetic reconnection problem. The algorithm can be easily extended to three dimensions, higher order accuracy, general geometries and parallel platforms.

Key words: Two-Fluid, Plasmas, Discontinuous Galerkin
PACS: Numerical methods
PACS: Plasma simulation

1 Introduction

Plasma physics continues to be an important area of numerical and experimental research. A number of magnetic confinement fusion concepts including spheromaks, FRCs, Z-pinches and inertial confinement concepts such as pellet implosion are under investigation at various facilities[1–4]. An important area of recent numerical research in plasma physics has been the development of plasma simulation algorithms with more complete physics including Hall MHD[5–10], quasi-neutral two-fluid MHD[11], and the full two-fluid model[12,13]. The full two-fluid algorithm presented in [12] is one dimensional and suffers large divergence errors when directly applied in 2D. In [13] a full electron-electron two-fluid algorithm using a

* Corresponding author. Address: jlovric@u.washington.edu
Email address: jlovric@u.washington.edu (J. Loverich).

combined spectral and finite difference approach is described for solving multi-dimensional problems in beam instabilities in ICF. In the current paper a discontinuous Galerkin (DG) method for the full ion-electron two-fluid plasma model is developed to provide a general multi-dimensional algorithm that works on arbitrary geometries and is highly parallelizable for solving problems of fusion interest. Because ion and electron masses differ this introduces different dynamics including the Hall effect and additional plasma time scales which are not observed in an electron-electron plasma.

The two-fluid equations retain electron inertia which simpler models such as Hall MHD lack. This term allows the electrons to become demagnetized and can provide dissipation in a collisionless plasma when resistivity is zero. The collisionless regime is particularly important to fusion plasmas. Electron inertia is important when reconnection processes which are ubiquitous in self organized plasmas. Charge separation and displacement current have been included for a more complete physical description.

2 Two-Fluid Model

The following definitions apply, electron and ion charges $\sigma_i = -\sigma_e = \sigma$ are equal, ion and electron mass are m_i and m_e. The speed of light is c and the permittivity is ϵ_0.

The two-fluid plasma model consists of a set of fluid equations for the electrons and ions plus the complete Maxwell's equations including displacement current.

$$\partial_t E - c^2 \nabla \times B = -\frac{1}{\epsilon_0} \sigma \left(n_i U_i - n_e U_e \right) \tag{1}$$

$$\partial_t B + \nabla \times E = 0 \tag{2}$$

$$\nabla \cdot B = 0 \tag{3}$$

$$\nabla \cdot E = \frac{\sigma}{\epsilon_0} \left(n_i - n_e \right) \tag{4}$$

The last two equations (3),(4) are constraint equations and are not solved numerically as they can be derived analytically from (1) and (2). Analytically the constraints are satisfied for all time if they are satisfied initially. Numerically, errors in the constraints may grow with time even if they are satisfied initially.

The fluid and electromagnetic systems are coupled through Lorentz forces and currents as source terms. Key things to note are that the displacement current is not neglected, electrons and ions have separate energy,

$$\partial_t e_s + \nabla \cdot \left(U_s \left(e_s + P_s \right) \right) = \sigma_s \, n_s E \cdot U_s \, , \tag{5}$$

momentum

$$\partial_t \left(\rho_s U_s\right) + \nabla \cdot \left(\rho_s U_s U_s\right) + \nabla P_s = \sigma_s \, n_s \left(E + U_s \times \, B\right) \, , \quad (6)$$

and continuity equations,

$$\partial_t \, \rho_s + \nabla \cdot \left(\rho_s U_s\right) = 0 \quad (7)$$

so each species has its own temperature, velocity and number density. This system is identical to the system used in [12].

Because the displacement current and charge separation are included this set of equations can be written as three systems of balance laws,

$$\frac{\partial \, q_e}{\partial t} + \nabla \cdot F_e \left(q_e\right) = \psi_e \left(q_e, \, q_{em}\right) \, , \quad (8)$$

for the electron fluid equations,

$$\frac{\partial \, q_i}{\partial t} + \nabla \cdot F_i \left(q_i\right) = \psi_i \left(q_i, \, q_{em}\right) \, , \quad (9)$$

for the ion fluid equations, and

$$\frac{\partial \, q_{em}}{\partial t} + \nabla \cdot F_{em} \left(q_{em}\right) = \psi_{em} \left(q_e, \, q_i\right) \, , \quad (10)$$

for Maxwell's field equations.

Keeping displacement current and charge separation means that for physical devices the time scales that must be resolved numerically are not computationally feasible. However, this issue is resolved by choosing the characteristic ratios as in [12] of the Debye length to plasma size, ion Larmor radius to plasma size and the ratio of ion thermal speed to speed of light to make our numerical solution feasible while still preserving the relevant physics.

3 Numerical Algorithm

Discontinuous Galerkin methods are high order extensions of upwind schemes using a finite element formulation where the elements are discontinuous at cell interfaces. Details of the method are applied to simple hyperbolic systems and the equations of inviscid gas dynamics are discussed in [14–17] and reproduced here for the two-fluid system with additional discussion of two-fluid specific issues. The balance law

$$\frac{\partial q}{\partial t} + \nabla \cdot F \left(q\right) = \psi \left(q\right) \quad (11)$$

is multiplied by the set of basis functions $\{v_r\}$ and integrated over the finite volume element K. For second order spatial accuracy the basis set

$$\{v_r\} = \{v_0, v_x, v_y\} = \{1, \frac{x - x_{i\,j}}{\frac{1}{2}\Delta\, x}, \frac{y - y_{i\,j}}{\frac{1}{2}\Delta\, y}\} \tag{12}$$

is used where $x_{i\,j}$ and $y_{i\,j}$ refer to the (x, y) coordinate at the center of the cell i, j. The equation is written,

$$\int \frac{\partial q}{\partial t}\, v_r\, dV + \int (\nabla \cdot F)\; v_r\, dV = \int \psi\, v_r\, dV\,. \tag{13}$$

Integrate by parts to get

$$\int_K \frac{\partial q}{\partial t}\, v_r\, dV + \int_{\partial\, K} (F \cdot n)\; v_r\, d\Gamma - \int_K F \cdot (\nabla\, v_r)\; dV = \int \psi\, v_r\, dV\,. \tag{14}$$

The discrete conserved variable q is defined as a linear combination of the basis functions inside an element K, with

$$q = \sum_r\; v_r\, q_r\,. \tag{15}$$

The integral $\int_K \frac{\partial q}{\partial t}\, v_r\, dV = \frac{\partial q_r}{\partial t}\, C\, V$ where C is the constant $\frac{1}{V}\int_K\; v_r^2\, dV$ and V is the volume of the element. Using these definitions the discrete equation becomes,

$$\frac{\partial q_r}{\partial t} C\, V + \sum_e \sum_l\; w_l\; (F \cdot n)\; v_r\, \Gamma_e - \sum_m\; w_m\, F \cdot (\nabla\, v_r)\; V = \sum_m\; w_m\, \psi\, v_r\, V\,, \tag{16}$$

when the integrals are replaced by appropriate Gaussian quadratures. Γ_e is the surface area of the cell face in consideration, e refers to an element face, l are quadrature points on a face and m are quadrature points in the volume. For a second order method the edge integrals are replaced by a two point Gaussian quadrature

$$\int_{-1}^{1} f\,(x)\, dx \approx f\left(\frac{1}{\sqrt{3}}\right) + f\left(-\frac{1}{\sqrt{3}}\right) \tag{17}$$

A four point quadrature is used for the volume integral given by,

$$\int_{-1}^{1}\int_{-1}^{1} f\,(x, y)\, dx \approx f\left(\frac{1}{\sqrt{3}}, \frac{1}{\sqrt{3}}\right) + f\left(-\frac{1}{\sqrt{3}}, \frac{1}{\sqrt{3}}\right) + f\left(-\frac{1}{\sqrt{3}}, -\frac{1}{\sqrt{3}}\right) + f\left(\frac{1}{\sqrt{3}}, -\frac{1}{\sqrt{3}}\right)\,. \tag{18}$$

The surface fluxes F are evaluated using an approximate Riemann flux while the volume fluxes are evaluated directly from the fluxes for either the fluid or Maxwell

systems. The discrete equations for the second order scheme are

$$\frac{\partial q_0}{\partial t} V + \sum_e \sum_l w_l \; (F \cdot n) \; v_0 \, \Gamma_e = \sum_m w_m \, \psi \, v_0 \, V \,, \quad (19a)$$

$$\frac{\partial q_x}{\partial t} V + 3 \sum_e \sum_l w_l \; (F \cdot n) \; v_x \, \Gamma_e - 3 \sum_m w_m \, F \cdot (\nabla \, v_x) \; V = 3 \sum_m w_m \, \psi \, v_x \, V \,, \quad (19b)$$

$$\frac{\partial q_y}{\partial t} V + 3 \sum_e \sum_l w_l \; (F \cdot n) \; v_y \, \Gamma_e - 3 \sum_m w_m \, F \cdot (\nabla \, v_y) \; V = 3 \sum_m w_m \, \psi \, v_y \, V \,. \quad (19c)$$

The derivatives of the basis functions can be calculated analytically since the polynomial basis functions are known. The discontinuous Galerkin method is applied to each balance law (8)(9)(10) at every time step. Third order TVD Runge-Kutta time integration is used.

The algorithm is stable if the plasma frequency is resolved and the Courant condition for the speed of light is satisfied. In one dimension the Courant condition is $c\frac{\Delta t}{\Delta x} < \frac{1}{3}$ and in 2D on a regular grid the condition is $c\frac{\Delta t}{\Delta x} < \frac{1}{6}$ where Δx is the grid spacing and Δt the time step.

3.1 Limiting

High resolution schemes typically use limiting to prevent spurious oscillations near discontinuities and for stabilization of non-linear systems. Limiters can also be used in the discontinuous Galerkin method, though instead of being TVD, limiters produce a scheme that is TVDM or TVD in the mean. This means that the solution is TVD in q_0, but not necessarily in q.

The conserved variables q can be limited in terms of characteristics. To limit q in terms of characteristics the q are first transformed to characteristic variables g where $g = L\,q$ and L is the left eigenvector matrix of the flux Jacobian calculated from q_0. The left eigenvector matrix is also applied to the differences $L\left(q_0^{i+1} - q_0^i\right) = \Delta^+ g_0$ and $L\left(q_0^i - q_0^{i-1}\right) = \Delta^- g_0$ where i refers to the ith cell. Limiting is performed directly on transformed variables and then the solution is immediately transformed

back to determine the limited form of q_x,

$$q_x^i = L^{-1}\,\bar{m}\left(g_x^i, \Delta^+ g_0, \Delta^- g_0, M\right) \tag{20}$$

where $\bar{m}$ is the modified minmod limiter defined by

$$\bar{m}\,(a,b,c) = \begin{cases} a & \text{if } |a| < M\,dx^2 \\ m\,(a,b,c) & \text{otherwise} \end{cases}, \tag{21}$$

and M is a constant while m is the minmod limiter.

$$m\,(a,b,c) = \begin{cases} \max(a,b,c) & \text{if sign}(a) = \text{sign}(b) = \text{sign}(c) = - \\ \min(a,b,c) & \text{if sign}(a) = \text{sign}(b) = \text{sign}(c) = + \\ 0 & \text{otherwise} \end{cases}. \tag{22}$$

For each of the fluid systems $M = 0$ to eliminate oscillations at shocks while for Maxwell's equations M is set to a constant that must be chosen empirically for each problem. TVB limiting of Maxwell's equations helps reduce divergence errors significantly over TVD limiters when approximate Riemann fluxes are used. Limiting is not necessary for the stability of Maxwell's equations since they are linear; unfortunately because of the coupling to the fluid equations through the Lorentz forces if no limiting is used for Maxwell's equations negative pressure problems frequently arise in the fluid equations.

4 GEM challenge comparison

In ideal MHD the fluid is frozen to the magnetic field lines and so field lines cannot reconnect without some non-ideal term. Resistivity allows field lines to reconnect though much slower than the fast reconnection that is observed in collisionless plasmas such as fusion and space plasmas. Since the accurate simulation of collisionless reconnection is a significant goal of this work the algorithm described is benchmarked against the GEM challenge simulations of [18], for which numerous plasma models have been tested. These results will not be discussed in detail in this paper as the primary scope is the novel numerical algorithm for the two-fluid plasma model.

In Fig. 1 the two-fluid solution is compared to solutions published in the GEM challenge papers [18,10]. The initial conditions are identical to those used in [18], but since displacement current is included the ratio of the speed of light to the maximum ion thermal velocity is specified $\frac{c}{v_{th\,i}} = 100$. Also open boundary conditions are used on the y boundaries instead of conducting walls. It is very easy to treat open boundaries with the discontinuous Galerkin method. The two-fluid solution

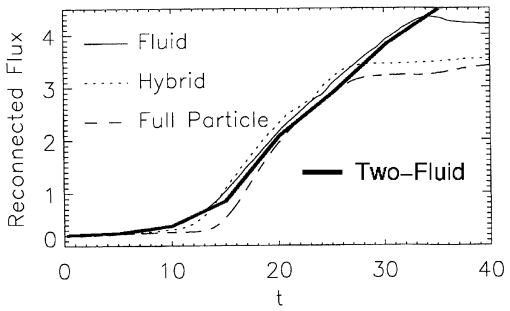

Fig. 1. Plot of reconnected magnetic flux vs time in units of inverse ω_{ci} published in [10]. The authors have overlayed the graph with the two-fluid solution calculated using the algorithm in this paper. The "Fluid" solution uses a simplified two-fluid approach that includes electron inertia effects.

shows good agreement with published solutions except that flux continues to reconnect in the two-fluid solution after it has saturated in the published solutions. The open y boundaries allow fluid and magnetic field lines to continue to flow in even after saturation occurs for conducting wall boundaries.

The full particle code of Fig.1 uses electron and ion particles with the full Maxwell's equations. The hybrid code uses ion particles with a modified Hall MHD description the electrons. The fluid code uses the same Hall MHD description as the hybrid code for the electrons, but uses fluid ions. The two-fluid solution was produced using the algorithm described in this paper on a 256×128 grid.

5 Conclusion

A discontinuous Galerkin method for the full two-fluid plasma model written as 3 balance laws has been described. The algorithm uses a second order spatial discretization and a 3rd order TVD Runge-Kutta time stepping scheme. The algorithm produces solutions to the GEM challenge magnetic reconnection problem that agree with published solutions. The algorithm can be extended to 3 dimensions, general geometries and to higher order accuracy.

This research was supported by AFOSR Grant No. F49620-02-1-0129. Computing resources were provided by the University of Washington Department of Mechanical Engineering through use of the Ladon cluster.

References

[1] P. M. Bellan, Spheromaks, Imperial College Press, 2000.

[2] H. Y. Guo, A. L. Hoffman, R. D. Brooks, A. M. Peter, Z. A. Pietrzyk, G. R. Votroubek, Formation and steady-state maintenance of field reversed configuration using rotating magnetic field current drive, Physics of Plasmas 9 185–200.

[3] U. Shumlak, R. P. Golingo, B. A. Nelson, D. J. D. Hartog, Evidence of stabilization in the z-pinch, Physical Review Letters 87 (20).

[4] J. D. Lindl, P. Amendt, R. L. Berger, S. G. Glendinning, S. H. Glenzer, S. W. Haan, R. L. Kauffman, O. L. Landen, L. J. Suter, The physics basis for ignition using indirect-drive targets on the national ignition facility, Physics of Plasmas 11 (2) (2004) 339–491.

[5] J. A. Breslau, S. C. Jardin, A parallel algorithm for global magnetic reconnection studies, Computer Physics Communications 151 (2003) 8–24.

[6] L. Chacon, D. A. Knoll, A 2d high-beta hall mhd implicit nonlinear solver, Journal of Computational Physics 188 (2003) 573–592.

[7] D. S. Harned, Z. Mikic, Accurate semi-implicit treatment of the hall effect in magnetohydrodynamic computations, Journal of Computational Physics 83 (1989) 1–15.

[8] A. Bhattacharjee, Center for magnetic reconnection studies: Present status, future plans, PSACI PAC Presentation, Princeton (June 2003).

[9] J. D. Huba, Hall magnetohydrodynamics - a tutorial, in: M. S. J. Buchner, C. T. Dunn (Ed.), Space Plasma Simulation, Springer, 2003, pp. 166–192.

[10] M. A. Shay, J. F. Drake, B. N. Rogers, R. E. Denton, Alfvenic collisionless magnetic reconnection and the hall term, Journal of Geophysical Research 106 (2001) 3759–3772.

[11] W. P. et. al., Plasma simulation studies using multilevel physics models, Physics of Plasmas 6 (5) (1999) 1796–1803.

[12] U. Shumlak, J. Loverich, Approximate riemann solver for the two-fluid plasma model, Journal of Computational Physics 187 (2003) 620–638.

[13] F. Califano, F. Pegoraro, S. V. Bulanov, Spatial structure and time evolution of the weibel instability in collisionless inhomogeneous plasmas, Physical Review E 56 (1) (1997) 963–969.

[14] B. Cockburn, C.-W. Shu, Tvb runge-kutta local projection discontinuous galerkin finite element method for conservation laws ii: General framework, Mathematics of Computation 52 (1989) 411–435.

[15] B. Cockburn, S.-Y. Lin, C.-W. Shu, Tvb runge-kutta local projection discontinuous galerkin finite element method for conservation laws iii: One-dimensional systems, Journal of Computational Physics 84 (1989) 90–113.

[16] B. Cockburn, S. Hou, C.-W. Shu, The runge-kutta local projection discontinuous galerkin finite element method for conservation laws iv: Multidimensional case, Mathematics of Computation 54 (1990) 545–581.

[17] B. Cockburn, C.-W. Shu, The runge-kutta discontinuous galerkin method for conservation laws v: Multidimensional systems, Journal of Computational Physics 141 (1998) 199–224.

[18] J. Birn, et al., Geospace environmental modeling (gem) magnetic reconnection challenge, Journal of Geophysical Research 106 (A3) (2001) 3715–3719.